RSC Advances

PAPER

View Article Online
View Journal | View Issue

Cite this: *RSC Adv.*, 2022, **12**, 26400

Intermolecular interactions of an isoindigo-based organic semiconductor with various crosslinkers through hydrogen bonding

Cuc Kim Trinh, *[a] Jin Woo Choi,[b] Thien Khanh Tran,[a] Zubair Ahmad [c] and Jae-Suk Lee *[d]

Received 19th August 2022
Accepted 5th September 2022

DOI: 10.1039/d2ra05190g

rsc.li/rsc-advances

Three crosslinkers (1,4-diaminobutane, 1,8-diaminooctane, and 1,6-hexanediol) were selected to produce hydrogen-bonded networks using a simple and effective method. The effects of these crosslinkers on the arrangement of crystalline structures were successfully studied using X-ray diffraction and high-voltage electron microscopy. The hydrogen-bonded isoindigo-based small molecules with 1,4-diaminobutane showed the best performance, with a crystal structure showing long-range order, due to the more suitable length of the 1,4-diaminobutane chain. The hole mobility estimated from hole-only devices based on isoindigo was enhanced from 1.24 × 10^{-6} cm^2 V^{-1} s^{-1} to 7.28 × 10^{-4} cm^2 V^{-1} s^{-1} as a result of the inclusion of this crosslinker, due to the formation of stronger interactions between the molecules.

Introduction

Intermolecular interactions are important in all aspects of chemistry and biochemistry. Commonly, hydrogen and other non-covalent interactions make supramolecular aggregates of organic molecules, which are used in various applications such as optoelectronic devices,[1,2] energy storage devices,[3–6] tissue engineering,[7] injectable delivery systems,[8] self-healing materials and hydrogels suitable for use as electrolytes, and artificial skin.[9–11] Bella *et al.* reported producing a self-healable cross-linked poly(urea-urethane) network by using polyethylene glycol 2000.[9] And Zhang *et al.* successfully designed a chitosan-based dual-network self-healing hydrogel formed *via* ionic hydrogen bonding and ionic crosslinking.[11]

In particular, interactions between molecules play a big role in defining the molecular order of organic semiconductors. The hydrogen bond is one of the most effective types of bonds participating in controlling intermolecular interactions and the order of molecules in organic semiconductors, and hence can enhance the optoelectrical properties of the semiconductors and charge carrier transport in the molecules. Hydrogen bonds can effectively improve the arrangement of molecules or crystal structures in the solid state.[12–14] New structural engineering approaches involving organic semiconductors or side chains attached to materials have been developed to form hydrogen bonds that boost the interactions between molecules.[15–17]

In recent years, isoindigo-based small molecules have constituted one of the most attractive candidates for use in optoelectronic devices such as photovoltaic devices, field-effect transistors and light-emitting diode.[18–22] Isoindigo has a highly planar structure with a strong N–H···C=O hydrogen bonding interaction that results in high crystallinity. These features are some of the major ones that enhance the performance of optoelectronic devices.[23–26]

Our group has been aiming to obtain well-organized isoindigo-based organic semiconductor thin films by generating hydrogen bonding. To do so, in previous work these highly ordered materials were treated thermally to remove the cleavable protecting groups[27,28] or crosslinked with ethylenediamine (EDA) crosslinkers to produce a hydrogen-bonded network.[29] However, the hole mobilities based on these materials were not as high as we had expected them to be, and not high enough for semiconductor Scheme 1 requirements. Therefore, in the current work, we designed new chemically engineered structures by using various crosslinkers to enhance the interactions between molecules. We did so based on the expectation of the chemical properties of the crosslinkers having a considerable ability to affect the interactions between the molecules.

Three crosslinkers, namely 1,4-diaminobutane, 1,8-diaminooctane and 1,6-hexanediol, were used to crosslink (*E*)-6,6′-di([2,2′-bithiophen]-5-yl)-1,1′-bis(2-ethylhexyl)-[3,3′-biindolilidene]-2-one (IID) to produce hydrogen-bonded networks. We investigated the effect of these crosslinkers *via* hydrogen bonding on controlling the arrangement of the molecules, the crystallinity of the resulting materials after the formation of hydrogen bonding as

[a]*Chemical Engineering in Advanced Materials and Renewable Energy Research Group, School of Engineering and Technology, Van Lang University, Ho Chi Minh City, Vietnam. E-mail: cuc.tk@vlu.edu.vn*

[b]*Department of Data Information and Physics, Kongju National University, 56 Gongjudaehak-ro, Gongju, Chungcheongnam-do 32588, Republic of Korea*

[c]*School of Chemical Engineering, Yeungnam University, 280 Daehak-ro, Gyeongsan, Gyeongbuk 38541, Republic of Korea*

[d]*School of Materials Science & Engineering, Gwangju Institute of Science and Technology (GIST), Gwangju 61005, Republic of Korea. E-mail: jslee@gist.ac.kr*

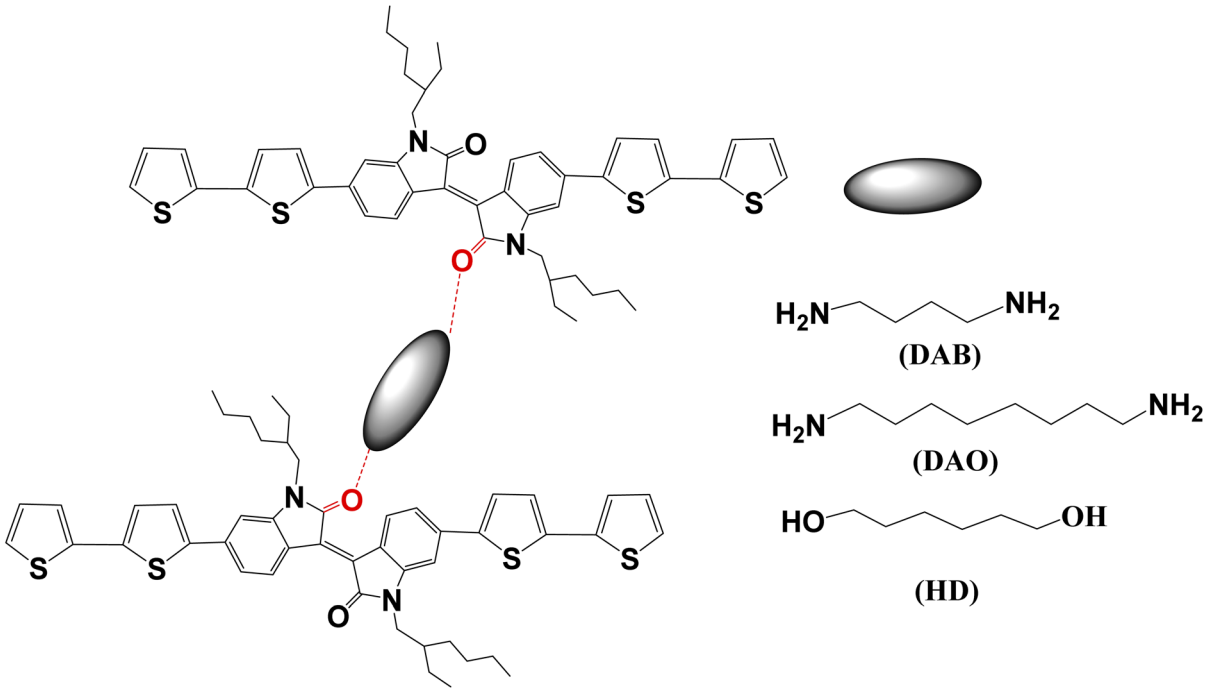

Scheme 1 The process of the formation of IID crosslinked with 1,4-diaminobutane (DAB), 1,8-diaminooctane (DAO), and 1,6-hexanediol (HD).

well as the hole mobility estimated from hole-only devices. We successfully controlled the molecular arrangement of small molecules by crosslinking them with these crosslinkers, and in this way were able to achieve improved hole mobility.

Experimental

Instruments and measurements

Film samples were spin-coated from a solution of 10 mg ml^{-1} of small molecules in chloroform onto glass plates. The arrangements and crystallinities of organic small molecules in the solid state before and after the formation of hydrogen bonding were studied by using a high-voltage electron microscope (HVEM, JEOL Ltd., JEM ARM 1300S, a point resolution of 0.12 nm). High-resolution transmission electron microscopy (HRTEM) images were acquired at 1250 kV (Gatan Inc., SP-US1000HV). X-ray diffraction measurements were taken using a Rigaku D/max-2500 diffractometer with Cu-K_α radiation ($\lambda = 1.54$ Å) at 40 kV and 100 mA.

Materials

2,2′-Bithiophene-5-boronic acid pinacol ester, 1,4-diaminobutane (DAB), 1,8-diaminooctane (DAO), and 1,6-hexanediol (HD) were purchased from the Sigma-Aldrich company. 6-Bromooxindole and 6-bromoissatin were purchased from Tokyo Chemical Industry. All materials were directly used without further purification. (*E*)-6,6′-Di([2,2′-bithiophen]-5-yl)-1,1′-bis(2-ethylhexyl)-[3,3′-biindolinylidene]-2-one (IID) was synthesized following our reported procedure.[22] IID was prepared by carrying out a Suzuki coupling reaction of 6,6′-dibrromo-*N*,*N*′-(2-ethylhexyl)-isoindigo with 2,2′-bithiophene-5-boronic acid pinacol ester.[22]

Crosslinking of isoindigo-based small molecules IID with various crosslinkers

The method used to crosslink IID small molecules followed our previously published work, but with other crosslinkers.[29] A mass of 10 mg of IID small molecules and a crosslinker, specifically 1.9 mg of 1,4-diaminobutane (DAB), 4 mg of 1,8-diaminooctane (DAO), or 3.2 mg of 1,6-hexanediol (HD), were individually dissolved in 1 ml of chloroform in 5 ml covered vials. The hydrogen-bonding of the IID small molecules was formed by the crosslinking between the isoindigo C=O groups with hydrogen atoms of these crosslinkers when the mixtures prepared above were mixed at 45 °C for 24 h, according to the literature.[29] Cut glass slides with dimensions of 15 mm × 15 mm were ultrasonically cleaned with deionized water, acetone and isopropyl alcohol for 15 minutes each, and then dried at 60 °C in an oven. The above mixtures were deposited onto these cleaned dried glass substrates. After this step, to increase the crystallinity, the resulting films were stored at room temperature for 24–48 h to slowly remove the solvent.

Fabrication and characterization of hole-only devices

Hole-only devices were fabricated by sandwiching synthesized organic material between two hole-transport layers containing electrodes. ITO substrates were commercially obtained and cleaned by sonicating them in DI water, acetone and isopropyl alcohol for 15 minutes. Subsequently, the ITO substrates were treated with a UV-ozone lamp for 10 minutes. Following this cleaning procedure, a 100-nm-thick PEDOT:PSS hole-transport

layer with a 1 to 1 ratio of Baytron AI4083 : PH1000 was fabricated using a spin coating method. The organic films each with one of various crosslinkers were formed by spin-coating a solution of 10 mg ml^{-1} of organic material in chloroform. Finally, onto each film, 5 nm of MoO_3 and 100 nm of Ag electrode were deposited through a shadow mask *via* thermal vacuum evaporation.

Results and discussion

Characterization of hydrogen bonded IID small molecules

Fourier-transform infrared (FT-IR) spectroscopy was used to investigate the expected hydrogen bonding interaction between the IID small molecules and the crosslinking materials. The FT-IR spectra acquired of IID before and after crosslinking are shown in Fig. 1. In non-crosslinked IID, an absorption band was observed at a wavenumber of 1716 cm^{-1}, related to the C=O stretching in the isoindigo moiety. This band shifted to 1686 cm^{-1} in the spectra of the DAB-, DAO- and HD-crosslinked materials; furthermore, new broad bands appeared at 3013–3627 cm^{-1} in each of these three cases. These results showed that the crosslinkers successfully reacted with oxygen-containing functional groups of the IID moiety and successfully generated N–H···O=C hydrogen bonding between IID small molecules and crosslinking materials.[29,30]

Effects of different crosslinkers on structural order and intermolecular distances of IID and crosslinkers

X-ray diffraction (XRD) measurements were taken to investigate the molecular arrangement and intermolecular distances of non-crosslinked IID and IID hydrogen-crosslinked with DAB, DAO or HD. Fig. 2 shows XRD patterns of the films having non-crosslinked and crosslinked IID. IID crosslinked with DAB *via* hydrogen bonding showed a high crystallinity with a new peak at $2\theta = 25.04°$ compared to non-crosslinked IID. There was also

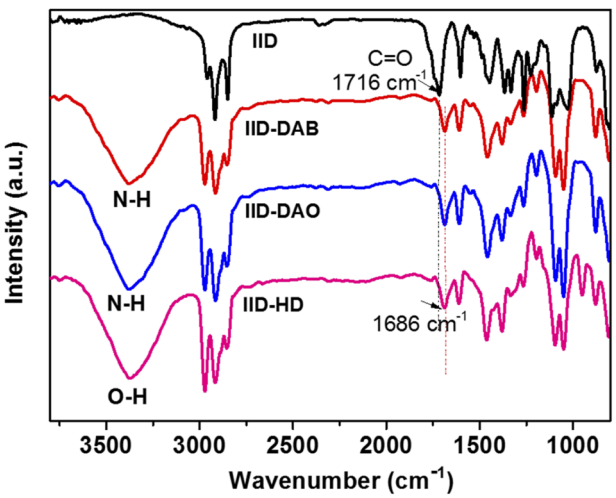

Fig. 1 FT-IR spectra of IID small molecules before any crosslinking and after crosslinking with 1,4-diaminobutane (DAB), 1,8-diaminooctane (DAO), and 1,6-hexanediol (HD), respectively.

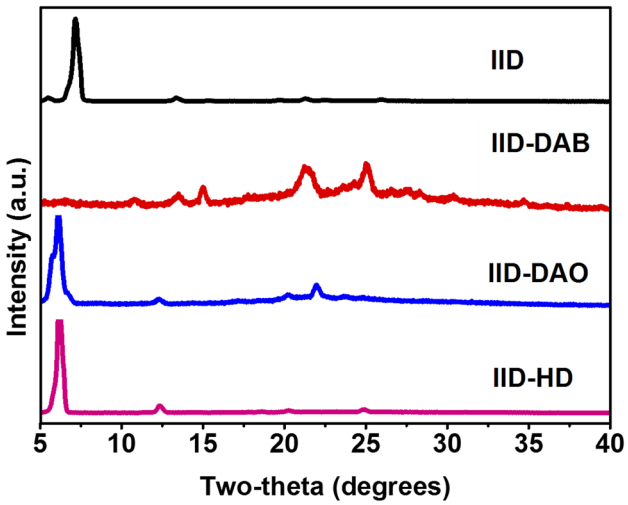

Fig. 2 X-ray diffraction patterns of samples of IID small molecules before and after they were crosslinked with 1,4-diaminobutane (DAB), 1,8-diaminooctane (DAO), and 1,6-hexanediol (HD), respectively.

successful suppression of the strong diffraction peak of the alkyl chain observed at 7.20° corresponding to a *d*-spacing of 1.23 nm. The new peak appeared related to an enhanced intermolecular interaction of the formed N–H···O=C hydrogen bonding as well as strong π–π interactions between molecules. This resulted in enhanced crystallinity of the films. However, its crystallinity was still lower than that of ethylenediamine (EDA)-crosslinked materials,[27] which may have been due to the flexibility of the linker molecules and different lengths of EDA and DAB. The crystallinities of DAO- and HD-crosslinked IID samples were much lower than that of IID–DAB. The strong peak observed at a two-theta (2θ) of 7.20° and related to the distance between the main backbones of conjugated IID separated by alkyl side chains of non-crosslinked IID was shifted to 6.1° (*d*-spacing of 1.45 nm) for DAO-crosslinked IID and 6.2° (*d*-spacing of 1.43 nm) for HD-crosslinked IID. The XRD results of IID crosslinked with DAO and HD still showed the presence of an alkyl–alkyl packing structure with increased *d*-spacings due to the greater chain lengths of the DAO and HD crosslinkers than of DAB.

The ordering of formed structures based on IID small molecules was further studied using high-voltage electron microscopy (HVEM), which can provide qualitative data on organic species.[31,32] As shown in Fig. 3a, without crosslinker showed relatively poor crystallinity with small crystal domains, perhaps due to steric hindrance of alkyl chain groups preventing effective π–π stacking between the main chains. In contrast, HRTEM images and the fast Fourier transforms (FFTs) of the IID crosslinked with DAB (IID–DAB) showed a structure exhibiting relatively long-range order (Fig. 3b). This enhancement of long-range order was attributed to the formation of N–H···C=O hydrogen bonding, specifically connecting hydrogens of the crosslinking material with oxygen-containing functional groups of the IID moiety. This hydrogen bonding apparently resulted in enhanced intermolecular interaction between molecules, which

nullified the effect of alkyl chain groups on the isoindigo moiety. From HRTEM images of IID–DAB, the *d*-spacing of 0.36 nm reflecting the length of molecules cross-linked by strong hydrogen bonding interactions was observed, and was in good agreement with the XRD peak at $2\theta = 25.04°$. In contrast to the HRTEM image of IID–DAB, those of DAO-crosslinked IID small molecules (IID–DAO) (Fig. 3c) and HD-crosslinked IID small molecules (IID–HD) (Fig. 3d) showed that their crystallinity levels were lower than that of IID–DAB. In addition, their crystal domains were too small to define the exact crystal structure. These differences may have been due to the greater flexibility of DAO and HD crosslinkers than of DAB resulting in reduced crystallinity of the films. The crystallinity levels of IID–DAO and IID–HD were poor, yet still suitable for observed HRTEM images.

Performance of a hole-only device of isoindigo-based small molecules

Since the DAB-introduced film showed a higher crystallinity than did the other examined crosslinked structures, an electronic study was performed on the IID–DAB film by using a hole-only device. The hole-only device provided charge carrier transport characteristics of a molecular-scale ordered IID film without and with DAB crosslinker. To compare the hole-mobility levels of IID and IID–DAB, 16 hole-only devices were fabricated for each sample in the same evaporation condition, and good reproducibility in the value of hole mobility was found. Fig. 4 presents the current density–voltage (*J*–*V*) performances of IID with and without DAB. Due to the asymmetry of the ITO/PEDOT:PSS/organic film/MoO_3/Ag device structure, the Fermi levels of PEDOT:PSS and MoO_3 resulted in a built-in internal field of approximately 0.2 V. Therefore, the measured *J*–*V* characteristics were compensated by this 0.2 V. The ohmic contact region and space charge limited conduction region were fitted by using the Mott–Gurney equation with a built-in voltage ($V_{\text{built-in}}$) correction term as

$$J = \frac{9}{8}\mu\varepsilon_s \frac{(V - V_{\text{built-in}})^2}{L^3},$$

where μ is the hole mobility, ε_s is material permittivity and L is the thickness of the organic film.[33–36] By assuming a dielectric constant of 3, the calculated hole mobilities of the IID film without and with 1,4-diaminobutane (IID–DAB) were 1.24×10^{-6} cm^2 V^{-1} s^{-1} and 7.28×10^{-4} cm^2 V^{-1} s^{-1}, respectively. That is, crosslinking was calculated to enhance the hole mobility about 600 fold. As observed with the XRD and TEM measurements, the mobility was improved due to the successful formation of a crystal structure showing long-range order. However, the hole mobility of IID–DAB was lower than expected, which might have been due to the substituted hexyl chain groups and/or crosslinkers increasing the insulation of the material.[37–39] Nevertheless, the hole mobility of IID–DAB was significantly enhanced compared to the material that was not crosslinked.

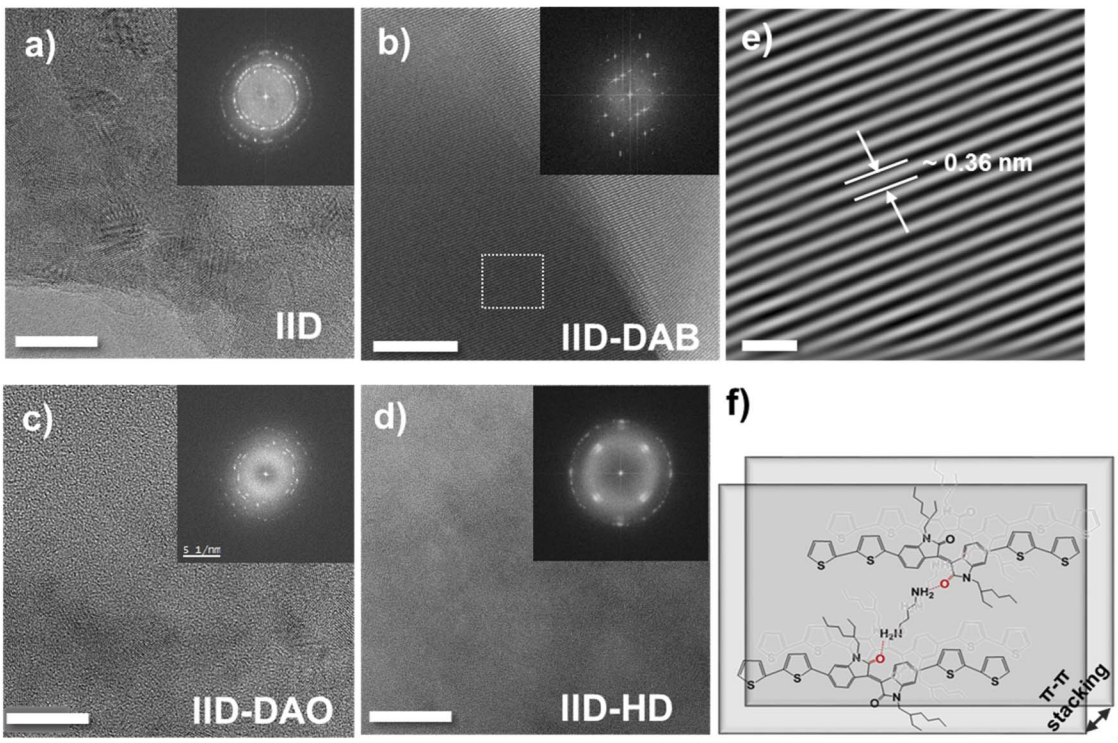

Fig. 3 HRTEM images of (a) IID before being subjected to crosslinking and (b) 1,4-diaminobutane (DAB)-, (c) 1,8-diaminoctane (DAO),- and (d) 1,6-hexanediol (HD)-crosslinked IID. The insets show the corresponding fast Fourier transform (FFT) images of each material. (e) An enlarged view of the portion of the image in panel (b) enclosed by a dotted square. Scale bars are 5 nm in (a–d) and 1 nm in (e). (f) A schematic illustration of the proposed chemical arrangement of IID crosslinked with DAB.

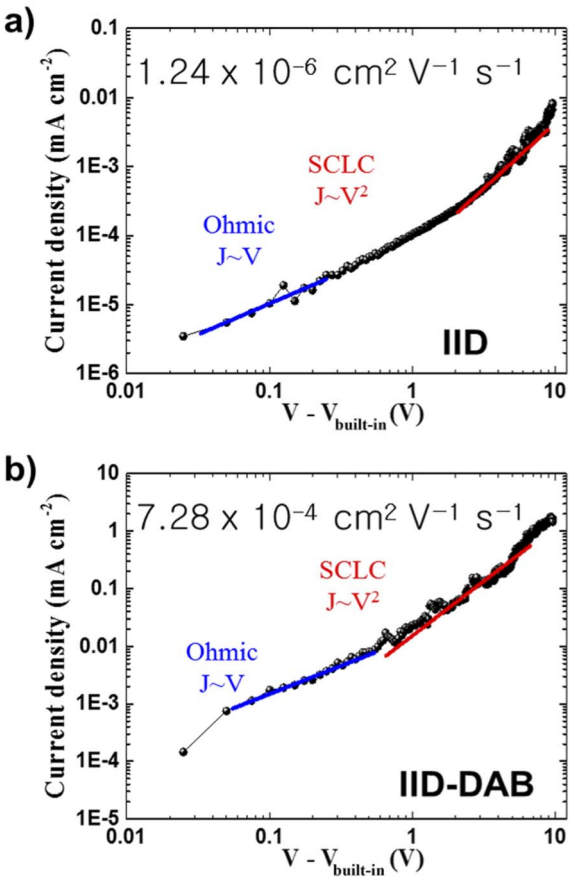

Fig. 4 *J*–*V* characteristics of a hole-only device with (a) IID and (b) IID–DAB. The red lines show fits to the Mott–Gurney law in the SCLC regime of device operation.

Conclusions

Three crosslinkers, namely 1,4-diaminobutane (DAB), 1,8-diaminooctane (DAO), and 1,6-hexanediol (HD), were used to hydrogen-bond IID small molecules to each other. The formation of crosslinking was confirmed based on the results of FT-IR measurements. The crystallinity levels of non-crosslinked IID and IID cross-linked with the three different crosslinkers were assessed from the inspection of HVEM images. Only DAB-crosslinked IID showed a good arrangement with long-range molecular order, with this result due to the suitable chain length of DAB crosslinkers. This crosslinking resulted in a significant change in morphology, crystallinity, and charge carrier transport properties. Although the hydrogen-bonded materials did not exhibit the expected high performance, they nevertheless showed increased hole mobility relative to that of the non-crosslinked material due to the advantage of crosslinking with suitable crosslinkers. This achievement, in the current work, of hydrogen-bonded organic materials displaying long-range order can inspire new avenues for simple and effective methods to design well-organized organic semiconductors for optoelectronic applications and for the study of molecular order.

Author contributions

C. K. Trinh: conceptualization, methodology, formal analysis, investigation, visualization, writing – original draft, review and editing, resources, supervision. J. W. Choi: investigation, methodology, formal analysis. T. K. Tran: writing – review and editing. Z. Ahmad: writing – review and editing. J.-S. Lee: writing – review and editing, resources, supervision.

Conflicts of interest

There are no conflicts to declare.

Acknowledgements

We thank Van Lang University, Vietnam for supporting the research.

References

1 J. C. d. Haro, E. Tatsi, L. Fagiolari, M. Bonomo, C. Barolo, S. Turri, F. Bella and G. Griffini, *ACS Sustainable Chem. Eng.*, 2021, **9**, 8550–8560.
2 N. A. Rahman, S. A. Hanifah, N. N. Mobarak, A. Ahmad, N. A. Ludin, F. Bella and M. S. Su'ait, *Polymer*, 2021, **230**, 124092–124204.
3 H. Yu, M. Bi, C. Zhang, T. Zhang, X. Zhang, H. Liu, J. Mi, X. Shen and S. Yao, *Electrochim. Acta*, 2022, **428**, 140908–140918.
4 H. Zhang, R. Zhang, F. Ding, C. Shi and N. Zhao, *Energy Storage Mater.*, 2022, **51**, 172–180.
5 Z. Ahmad, W. Kim, S. Kumar, T.-H. Yoon, J.-J. Shim and J.-S. Lee, *Electrochim. Acta*, 2022, **415**, 140243–140251.
6 J. H. Kim, Z. Ahmad, Y. Kim, W. Kim, H. Ahn, J.-S. Lee and M.-H. Yoon, *Chem. Mater.*, 2020, **32**, 8606–8618.
7 P. Y. W. Dankers, M. C. Harmsen, L. A. Brouwer, M. J. A. V. Luyn and E. W. Meijer, *Nat. Mater.*, 2005, **4**(7), 568–574.
8 P. Y. W. Dankers, T. M. Hermans, T. W. Baughman, Y. Kamikawa, R. E. Kieltyka, M. M. C. Bastings, H. M. Janssen, N. A. J. M. Sommerdijk, A. Larsen, M. J. A. Van Luyn, A. W. Bosman, E. R. Popa, G. Fytas and E. W. Meijer, *Adv. Mater.*, 2012, **24**, 2703–2709.
9 F. Elizalde, J. Amici, S. Trano, G. Vozzolo, R. Aguirresarobe, D. Versaci, S. Bodoardo, D. Mecerreyes, H. Sardon and F. Bella, *J. Mater. Chem. A*, 2022, **10**, 12588–12596.
10 E. Manarin, F. Corsini, S. Trano, L. Fagiolari, J. Amici, C. Francia, S. Bodoardo, S. Turri, F. Bella and G. Griffini, *ACS Appl. Polym. Mater.*, 2022, **4**, 3855–3865.
11 M. Kang, S. Liu, O. Oderinde, F. Yao, G. Fu and Z. Zhang, *Mater. Des.*, 2018, **148**, 96–103.
12 H. Zhang, K. Liu, K.-Y. Wu, Y.-M. Chen, R. Deng, X. Li, H. Jin, S. Li, S. S. C. Chuang, C.-L. Wang and Y. Zhu, *J. Phys. Chem. C*, 2018, **11**, 5888–5895.
13 Z. Deng, K. Yang, L. Li, W. Bao, X. Hao, T. Ai and K. Kou, *Dyes Pigm.*, 2018, **151**, 173–178.

14 H. Zhang, R. Li, Z. Deng, S. Cui, Y. Wang, M. Zheng and W. Yang, *Dyes Pigm.*, 2020, **181**, 108552–108558.
15 C. K. Trinh and N. I. Abdo, *J. Mol. Struct.*, 2022, **1269**, 133764.
16 K.-H. Kim, H. Yu, H. Kang, D. J. Kang, C.-H. Cho, J. H. Oh and B. J. Kim, *J. Mater. Chem. A.*, 2013, **1**, 14538–14547.
17 I. D. Tevis, L. C. Palmer, D. J. Herman, L. P. Murray, D. A. Stone and S. I. Stupp, *J. Am. Chem. Soc.*, 2011, **133**, 16486–16494.
18 J. Mei, K. R. Craham, R. Stalder and J. R. Reynolds, *Org. Lett.*, 2010, **12**, 660–663.
19 M. Shaker, J.-H. Lee, C. K. Trinh, W. Kim, K. Lee and J.-S. Lee, *RSC Adv.*, 2015, **5**, 66005–66012.
20 M. Karakawa and Y. Aso, *RSC Adv.*, 2013, **3**, 16259–16263.
21 A. Yassin, P. Leriche, M. Allain and J. Roncali, *New J. Chem.*, 2013, **37**, 502–507.
22 W. Elsawy, C.-L. Lee, S. Cho, S.-H. Oh, S.-H. Moon, A. Elbarbary and J.-S. Lee, *Phys. Chem. Chem. Phys.*, 2013, **15**, 15193–15203.
23 M. S. Yuan, Q. Fang, L. Ji and W. Yu, *Acta Crystallogr., Sect. E: Struct. Rep. Online*, 2007, **63**, o4342.
24 M. A. Naik and S. Patil, *J. Polym. Sci., Part A: Polym. Chem.*, 2013, **51**, 4241–4260.
25 E. Wang, W. Mammo and M. R. Andersson, *Adv. Mater.*, 2014, **26**, 1801–1826.
26 E. Wang, Z. Ma, Z. Zhang, K. Vandewal, P. Henriksson, O. Inganäs, F. Zhang and M. R. Andersson, *J. Am. Chem. Soc.*, 2011, **36**, 14244–14247.
27 C. K. Trinh, H.-J. Lee, J. W. Choi, M. Shaker, W. Kim and J.-S. Lee, *New J. Chem.*, 2018, **42**, 2557–2563.
28 C. K. Trinh, J. W. Choi, H.-J. Lee, M. Shaker, W. Kim, C.-L. Lee and J.-S. Lee, *Synth. Met.*, 2018, **246**, 172–177.
29 C. K. Trinh, J. W. Choi, W. Kim and J.-S. Lee, *Synth. Met.*, 2019, **256**, 116149–116154.
30 I. V. Rubtsov, K. Kumar and R. M. Hochstrasser, *Chem. Phys. Lett.*, 2005, **402**, 439–443.
31 M. H. Loretto and R. E. Smallman, *Mater. Sci. Eng.*, 1977, **28**, 1–32.
32 R. F. Egerton, P. Li and M. Malac, *Micron*, 2004, **35**, 399–409.
33 W. Chandra, L. K. Ang, K. L. Pey and C. M. Ng, *Appl. Phys. Lett.*, 2007, **90**, 153505–153507.
34 M. Kiy, P. Losio, I. Biaggio, M. Koehler, A. Tapponnier and P. Gunter, *Appl. Phys. Lett.*, 2002, **80**, 1198–1200.
35 J. Hwang, A. Wan and A. Kahn, *Mater. Sci. Eng., R*, 2009, **64**, 1–32.
36 A. Kahn, N. Koch and W. Gao, *J. Polym. Sci., Part B: Polym. Phys.*, 2003, **41**, 2529–2548.
37 R. J. Kline and M. D. McGehee, *J. Macromol. Sci., Part C: Polym. Rev.*, 2006, **46**, 27–45.
38 A. Salleo, *Mater. Today*, 2007, **10**, 38–45.
39 B. Kang, B. Moon, H. H. Choi, E. Song and K. Cho, *Adv. Electron. Mater.*, 2016, **2**, 1500380–1500387.